JOURNAL OF MATERIALS SCIENCE **36** (2001) 4485–4491

Studies on compressive failure features in syntactic foam material

N. GUPTA*
Department of Mechanical Engineering, Louisiana State University, Baton Rouge, LA 70803, USA
E-mail: nikgupt@yahoo.com

KISHORE
Department of Metallurgy, Center for Advanced Studies, Polymer Composite Laboratory, Indian Institute of Science, Bangalore 560 012, India

E. WOLDESENBET
Department of Mechanical Engineering, Louisiana State University, Baton Rouge, LA 70803, USA

S. SANKARAN
Aeronautical Development Establishment, C.V. Raman Nagar, Bangalore 560 093, India

Syntactic foam made by mechanical mixing of glass hollow spheres in epoxy resin matrix is characterized for compressive properties in the present study. Volume fraction of hollow spheres in the syntactic foam under investigation is kept at 67.8%. Effect of specimen aspect ratio on failure behavior and stress-strain curve of the material is highlighted. Considerable differences are noted in the macroscopic fracture features of the specimen and the stress-strain curve with the variation in specimen aspect ratio, although compressive yield strength values were within a narrow range. Post compression test scanning electron microscopic observations coupled with the macroscopic observations taken during the test helped in explaining the deviation in specimen behavior and in gathering support for the proposed arguments.

1. Introduction

Developed in early 60's as buoyancy-aid materials for deep-sea applications [1], syntactic foams soon gained attention of aeronautical sector due to their superior compressive properties and adaptability to many situations through the use of various reinforcements and filler materials. The possibilities of making wide range of densities including the very low value bearing ones are the key to these materials gaining increasing attention. Among other properties low radar detectability and low moisture absorption [2] open a route for these materials for structural applications in the aeronautical sector. Depending upon raw materials and the composition, it is possible to manufacture syntactic foams having compressive yield strength between 10 to 100 MPa and density range from 150 to over 1000 kg/cm^3.

Due to the presence of hollow spheres in the syntactic foam structure, porosity is present in the closed cell form. The hollow spheres may be made up of metals, polymers or ceramics [3]. Similarly several types of polymers are used as matrix resin [4]. If the hollow spheres are incorporated to the maximum possible volume fraction, they are expected to assume a close packed structure. For this reason the word "syntactic" is used for this class of materials [1]. Fig. 1A illustrates the schematic appearance of two- phase structure, while Fig. 1B depicts the situation corresponding to three-phase structure [5]. Presence of air in the structure of syntactic foam other than in the hollow spheres is expected to be negligible leading it to come under the purview of a two-phase structure.

Syntactic foams are normally used as cores in the sandwich configurations in a large number of applications and provide superior properties compared to other conventionally used core materials. In such configurations, their ability to keep the damage highly localized has been used to design damage tolerant structures and components. Impact properties of syntactic foam core sandwich structured composites are studied by Ishai *et al.* [6, 7].

Reports on compressive studies of the syntactic foam were found in the literature from the works of Puterman *et al.* [2], Bunn and Mottram [8] and Sankaran [9]. Reviews published by Shutov [3, 10] give details of preparation and properties of polymeric syntactic foams. The reports highlight, among other observations, a general

* Author to whom all correspondence should be addressed.

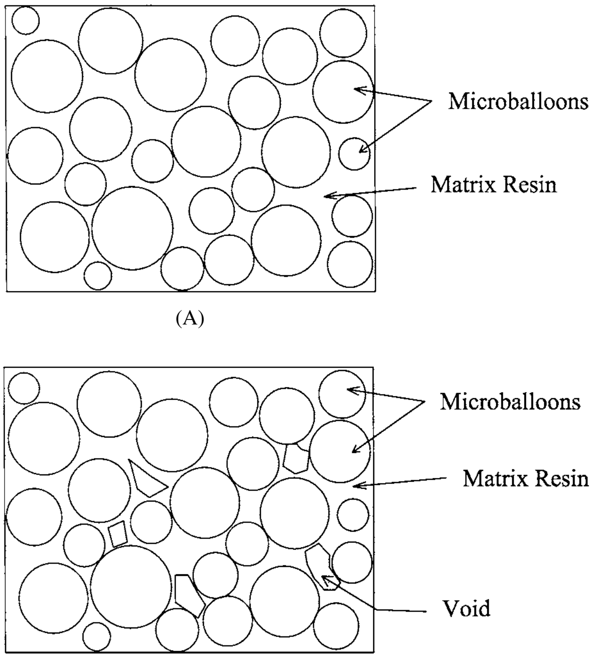

Figure 1 Schematic showing the features in (a) two phase and (b) three phase structures in a syntactic foam material.

stress-strain curve for a low hollow sphere volume fraction bearing syntactic foam system. In the present study stress is laid on analyzing the compressive properties of high hollow sphere volume fraction bearing two-phase syntactic foam system. Volume fraction of glass hollow spheres in the fabricated syntactic foam slabs was maintained at 74%. Further on, compressive properties with respect to the aspect ratio (height/width ratio) of the test specimens were looked into. The investigation was carried out with an aim of looking at the deformation and fracture features of syntactic foam specimens in the compressive loading conditions, shape of stress–strain curve and compressive strength values arising from alteration in aspect ratio of the specimen. Attempts have been made to correlate the different factors at various stages of compression testing.

2. Materials

The raw materials used to fabricate syntactic foam were glass hollow spheres (microballoons) as closed pore material and epoxy resin as matrix system. Glass microballoons supplied by Grace Electronic Materials (Belgium) had an average particle diameter of 80 μm and bulk density of 254 kg/m^3. Glass microballoon particle size distribution and compressive strength values provided by the supplier are given in Tables I and II respectively. Low temperature curing epoxy resin (LY

TABLE I Particle size distribution of glass microballoons

No.	Particle size range (μm)	Weight fraction
1	149–175	0.14
2	125–149	0.10
3	100–125	0.12
4	44–100	0.55
5	<44	0.09

TABLE II Crushing strength of glass microballoons

No.	Stress level (MPa)	% Collapse
1	3.4	14
2	6.9	32
3	13.8	55
4	20.7	75

5052) with the hardener (HY 5052), manufactured by Ciba-Geigy was used as the matrix material. Resin system had a density of 1100 kg/m^3. Resin and hardener were mixed together in the ratio of 100:38 by weight. For the fabrication of syntactic foam slabs, resin system to microballoon ratio of 1.52:1 by weight was taken, which is 74.0% microballoons and 26.0% resin by volume. Density of the foam slabs was 433 kg/m^3 with a variation of 0.18% among the various slabs. Average void content (open cell porosity) in the foam slab was 8.4% by volume, with a variation of 0.2% among various foam slabs. Through careful and extensive scanning electron microscopy it was observed that the voids were evenly distributed in the structure. Due to the voids in the structure the final volume fractions of the materials in the syntactic foam slabs can be given as: resin 23.8%, microballoons 67.8% and voids 8.4%. Through a careful processing schedule and repetition of experiments, the above cited value for the void content was found to be the minimal approachable for the given combination of materials and the processing parameters.

Syntactic foam was cast as slabs in the mold of dimensions measuring $150 \times 150 \times 25.4$ mm^3 by unpressurized casting. Foam slabs were cured for 18 hrs at ambient temperature and then post cured at 130 ± 3°C for 2 1/2 hrs.

3. Test parameters

A 100 KN DARTEC-9500 servo-hydraulic microprocessor controlled machine was used for carrying out the compression tests. True strain rate of 0.01 s^{-1} was maintained throughout the test. Load vs. displacement data plots obtained from the test were used for the analysis.

Based on the cellular structure of the materials, ASTM D1621 [11] test standard was considered to be suitable for compression tests. In order to investigate the effect of specimen aspect ratio on the compressive test results, several aspect ratio values were taken within the range recommended in this ASTM standard. A smaller than ASTM recommended specimen cross-section area specimens were fabricated and tested. This is justified by the fact that the average cell size in the material is 80 microns and about 75% of the microballoons had size less than 125 microns, hence over 75 cells would be present in the smallest dimension of any of the test specimens, which is 10 mm. Due to presence of large number of cells in the specimen in any given direction the effect of localized phenomena, if any, is expected to be negligible. The characterization of syntactic foam for the mechanical data with respect to the specimen aspect ratio has not been found explored in the literature.

TABLE III Values of compressive yield strength for the syntactic foam specimens

Specimen type	Dimensions (mm) $h \times l \times b^*$	Aspect satio	Compressive yield strength (MPa)
A	10 × 11 × 11	0.91	22.4
B	10 × 15 × 15	0.67	20.5
C	6.0 × 10 × 10	0.6	19.7
D	10 × 25 × 25	0.4	20.9

*h, l and b are height, length and width of the specimens respectively.

4. Experimental

Square cross section area specimens were prepared from the cast foam slabs for testing. Specimens having four different aspect ratios 0.91, 0.67, 0.6 and 0.4 were fabricated for compression testing. Dimensions of all the specimens tested in this study are given in Table III. Variations in the measurements of the dimensions of the specimens were kept below the ASTM standard recommended value of 1%.

In order to make this characterization study more complete, the behavior of the specimen and the occurrence of various events during the test were carefully monitored. Tests were continued well beyond the minimum recommended compression value, which is 13% or the appearance of yield point. Compressive yield strength was measured for every specimen. For the specimens that did not show a distinct yield point, tangents were drawn to the linear portions of elastic region and plastic region of the curve. The intersection point of these tangents was taken as the yield point for that specimen.

5. Results and discussion

For the syntactic foam material under investigation in the present study the test standard ASTM D 1621-94 is considered suitable. In an earlier study of low microballoon volume fraction syntactic foams [8], the specimens having aspect ratio of 2 were tested according to the test standard ASTM D 695-91 [12]. For low volume fraction of the microballoons, the characteristics of epoxy resin matrix prevail and this standard, which is for compression testing of rigid plastics, can be followed. At higher volume fraction of microballoons the syntactic foam material behaves like a cellular material having cell size equal to the size of microballoons. Hence, the standard ASTM D 1621-94, which is specifically for cellular structured rigid plastics, is followed. It is of relevance to note that with total porosity figure (open and closed porosity combined) being as high as 76%, specimens having aspect ratio value of 1 or higher display difficulties in uniform compression. This is due to the formation of powdery and loose mass at the region where crack originated in the early stages of compression, which later on leads to the separation of fragments from the material around the path of the crack. For this reason it was decided not to try out aspect ratios of 1 for the studies and the maximum value of aspect ratio was set at 0.91. The values of specimen aspect ratios taken in this study are in the range recommended by ASTM D 1621-94. Justification for taking smaller cross-section area than the recommended values is given in test parameters sections.

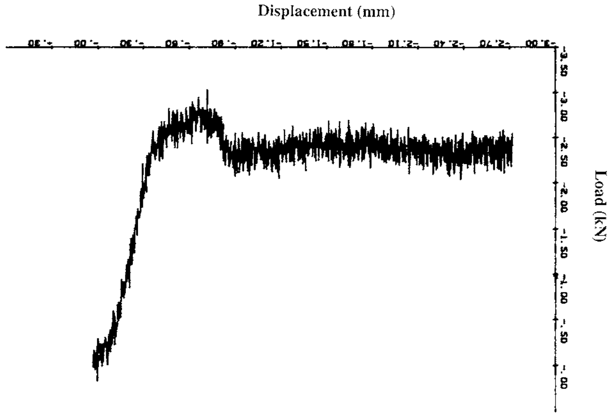

Figure 2 Load-displacement curve for high aspect ratio (0.91) syntactic foam specimen as obtained during the compression test.

An actual load-displacement curve obtained in the compression testing of the specimen having aspect ratio of 0.91 is shown if Fig. 2. A generalized schematic curve for the specimens having the higher side of values for aspect ratio (viz., 0.91 and 0.67) is shown in Fig. 3, where a distinct yield point at the end of elastic region could be noted. The decrease in the load at this point was of the order of about 15 to 20% of the peak load. This curve is divided into three distinct regions. Region 1 showing linear trend corresponds to the elastic behavior of the foam. At the end of the region 1, a yield point is seen and the load becomes nearly constant after a slight decrease, which is termed as region 2 or plateau region. At the end of the second region stress again starts increasing. Plateau region corresponds to the energy absorption in the process of crushing of microballoons. Hollow space exposed by the fracture of microballoons is consumed by the materials while getting compressed. When a significant fraction of microballoons gets crushed, further increase in the load results in the densification of the foam and is visible as an upward trend in the curve. Similar observations were made by Bunn and Mottram [8] also. On the contrary, the specimens having a lower value of aspect ratio, namely 0.6, did not display this decrease in stress after the maximum value. Stress becomes nearly

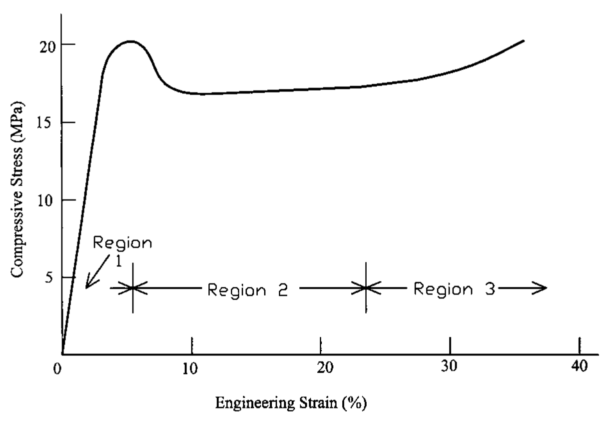

Figure 3 Generalized stress-strain curve for high aspect ratio bearing syntactic foam specimens.

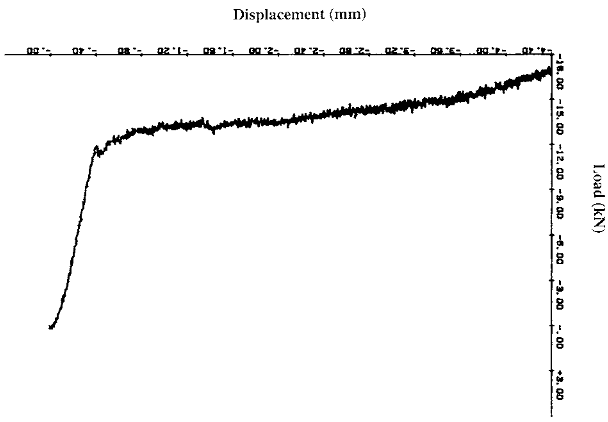

Figure 4 Load-displacement curve for low aspect ratio (0.4) syntactic foam specimen as obtained during compression test.

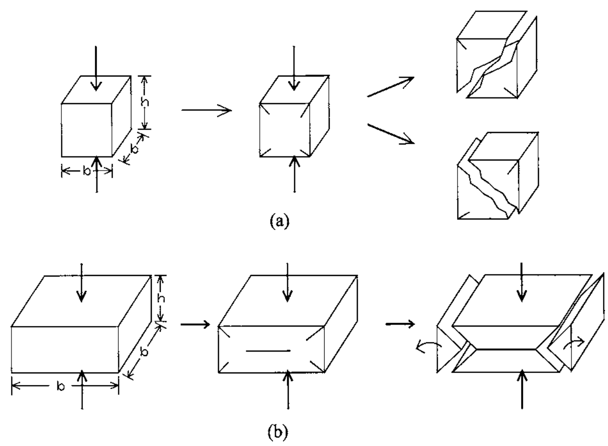

Figure 6 Schematic representation of crack origination and propagation sequence in (a) high aspect ratio and (b) low aspect ratio specimens.

constant at this value in the plateau region and starts increasing rapidly after the densification is complete. This was the first major deviation stressing the need for further investigation and interpretation based on observations both in-situ and post-compression fractography. To continue the effort for confirmation of the occurrence of such a trend, specimens having lower aspect ratio (0.4) were tested and it was observed that these show continuous increase in stress as shown in Fig. 4, which is an actual load-displacement curve obtained in the testing. There is no decrease in load value at any point in this curve. Fig. 5 schematically represents a generalized curve for such specimens. These observations reinforce the contention that characterizing and correlating the mechanical test data with test parameters is a critical and essential aspect of this type of emerging aerospace material.

Values of compressive yield strength for various specimen dimensions and aspect ratios are listed in Table III. Slight difference in values can be observed as the aspect ratio becomes higher and tends towards the value of 0.91, the maximum value taken in this study. However, even in such extreme cases the difference is less than 10%. A possible source for this discrepancy to arise may be the fact that two different methods, as mentioned in the Experimental section, are used for the calculation of compressive yield strength due to two different shapes of the stress-strain curves and absence of yield point in one case.

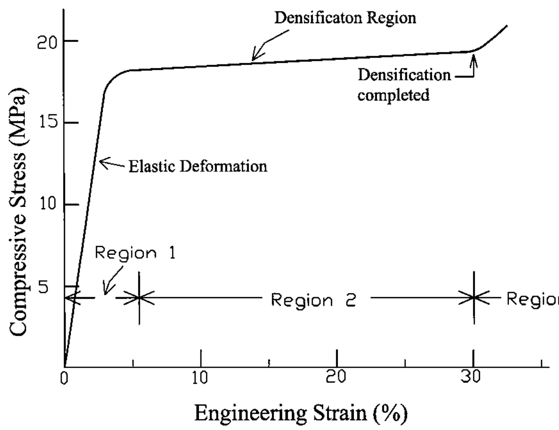

Figure 5 A generalized stress-strain curve suggested for low aspect ratio bearing syntactic foam specimens containing high volume fraction of microballoons.

One possible way to explain the above observations is to examine the behavior of specimens during testing followed by recording post compression micro and macroscopic features in all of the cases. In contrast to the compressive yield strength values, the specimen behavior during compression shows remarkable difference with respect to the aspect ratio. It was first observed that shear type of cracks originate at the corners of the specimen. In specimens having high aspect ratio that possess sufficient thickness, the cracks propagate through the specimen center to the opposite face, giving rise to shear type of failure (Figs 6a and 7). However, a similar crack propagation event yielded wedge-shaped fragments from the sidewalls in the low aspect ratio specimens (Figs 6b, 8 and 9). Also, a large central part of the specimen remained intact and compressed uniformly.

Formation of fragments at the sidewall of low aspect ratio specimens can be understood by analyzing the stress conditions in the specimens. The stress tensor for uniaxial compressive state of stress can be given as:

$$\sigma_{ij} = \begin{bmatrix} -\sigma & 0 & 0 \\ 0 & 0 & 0 \\ 0 & 0 & 0 \end{bmatrix} \tag{1}$$

where σ is the applied stress. This stress can be divided into hydrostatic (σ_{hyd}) and deviatoric (σ_{dev}) stress components [13].

$$\sigma_{ij} = \sigma_{\text{hyd}} + \sigma_{\text{dev}} \tag{2}$$

where σ_{hyd} and σ_{dev} can be given as:

$$\sigma_{\text{hyd}} = \begin{bmatrix} -\frac{\sigma}{3} & 0 & 0 \\ 0 & -\frac{\sigma}{3} & 0 \\ 0 & 0 & -\frac{\sigma}{3} \end{bmatrix}$$

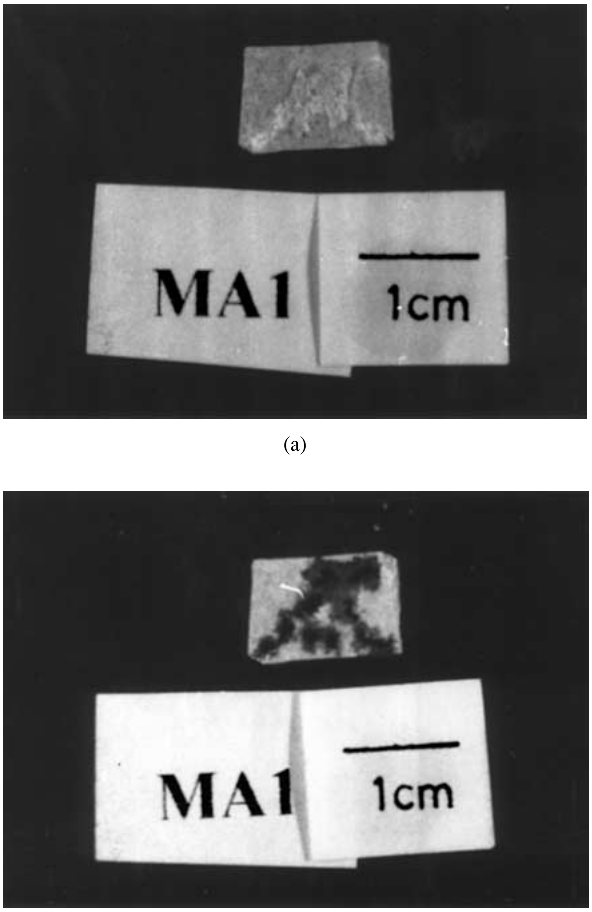

(a)

(b)

Figure 7 Macroscopic view showing elevation in a high aspect ratio (0.9) compressed specimen showing cracks (a) without and (b) with decoration with a dye penetrant. Note the continuous crack running for most part of the diagonal in the latter.

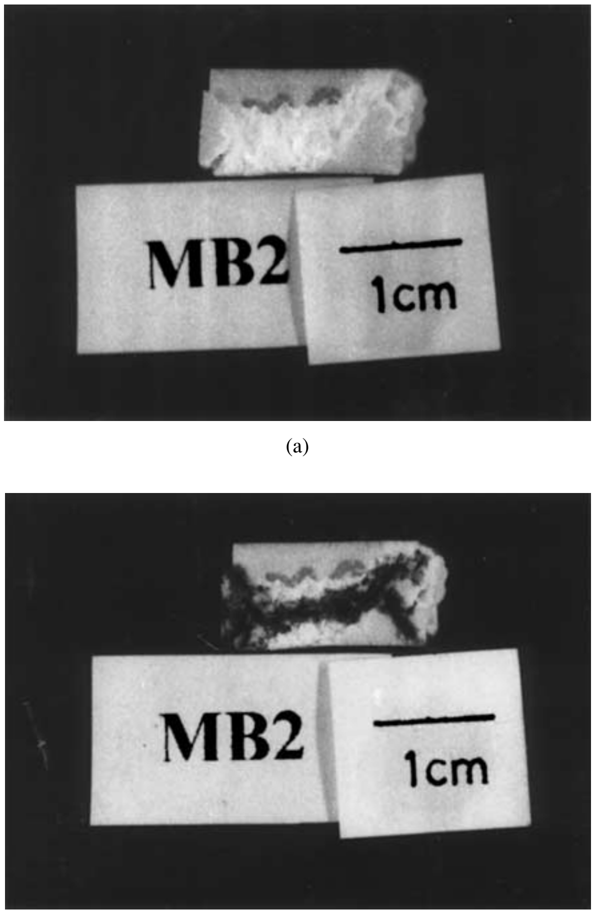

(a)

(b)

Figure 8 A 0.67 aspect ratio specimen displaying features in the same specimen (a) before and (b) after decoration with a dye penetrant. Note the wedge formation on either side of the latter figure.

and

$$\sigma_{\text{dev}} = \begin{bmatrix} -\frac{2\sigma}{3} & 0 & 0 \\ 0 & \frac{\sigma}{3} & 0 \\ 0 & 0 & \frac{\sigma}{3} \end{bmatrix}$$

Hydrostatic part of the stress tensor shown above produces only elastic deformation in the specimen. It does not contribute to the plastic deformation. Deviatoric stress component of the stress tensor produces plastic deformation and can further be divided into two parts, both representing a state of pure shear.

$$\begin{bmatrix} -\frac{2\sigma}{3} & 0 & 0 \\ 0 & \frac{\sigma}{3} & 0 \\ 0 & 0 & \frac{\sigma}{3} \end{bmatrix} = \begin{bmatrix} -\frac{2\sigma}{3} & 0 & 0 \\ 0 & \frac{2\sigma}{3} & 0 \\ 0 & 0 & 0 \end{bmatrix} + \begin{bmatrix} 0 & 0 & 0 \\ 0 & -\frac{\sigma}{3} & 0 \\ 0 & 0 & \frac{\sigma}{3} \end{bmatrix} \quad (3)$$

Hydrostatic component of applied compressive stress is responsible for compressive stress while deviatoric part gives rise to shear stresses in the material. In the case of syntactic foams compressive strength of microballoons vary over a wide range of values with particle size as the particle diameter to cavity diameter ratio changes. Fracture of microballoons starts at very low stress levels. At stress as low as 3.45 MPa 14% microballoons fracture (Table II). Fracture of microballoons leaves behind a cavity of substantial size. Due to the high volume fraction of microballoons (67.8% in the structure of syntactic foam), the layer of matrix resin between microballoons is very thin and it tends to fracture easily under shear stresses. Fracture under secondary tensile stresses is less likely as tensile strength of epoxy resin is higher than its shear strength [14] and the separation of wedge shaped fragments happens along the planes of maximum shear stress.

In high aspect ratio bearing specimens, cracks originating from opposite corners tend to meet and give rise to fracture of specimen apparently in shear mode. On the contrary, in low aspect ratio specimens after initial separation of fragments due to shear stress components along the planes of maximum shear stress, rest of the material is primarily subjected to the compressive forces. During this period two mutually competing processes, namely fracture of microballoons exposing empty space existing inside them and compaction of material balance each other, which is reflected as plateau region in the stress strain curve.

Scanning electron micrograph taken from the center of a uniformly compressed specimen of low aspect ratio (0.6) specimen shows large amount of fractured pieces of microballoons (Fig. 10). The fractured microballoons appear as debris and are a typical feature of failure under compression.

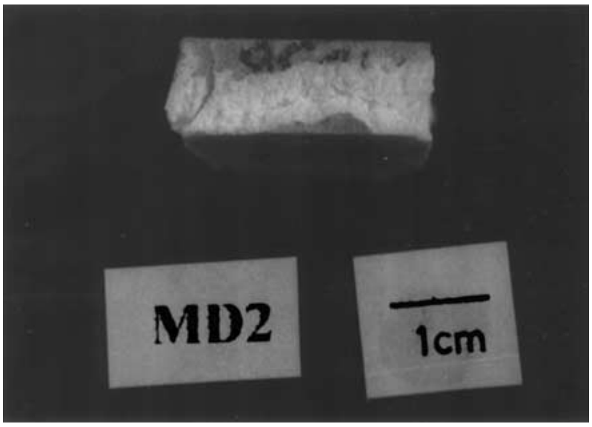

(a)

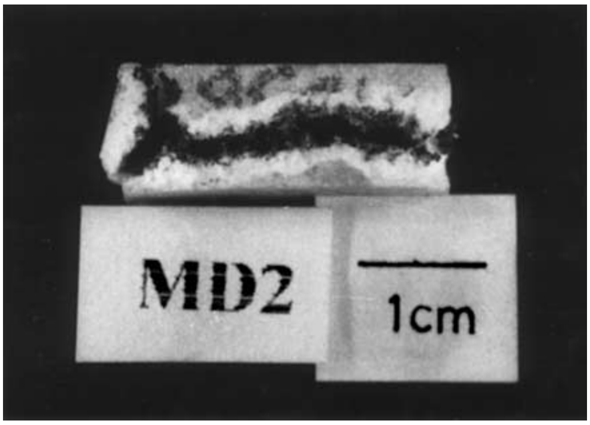

(b)

Figure 9 Features seen with still lower (0.4) aspect ratio (a) without (b) with decoration with a dye penetrant. Note the presence of wedge on the left side of the specimen.

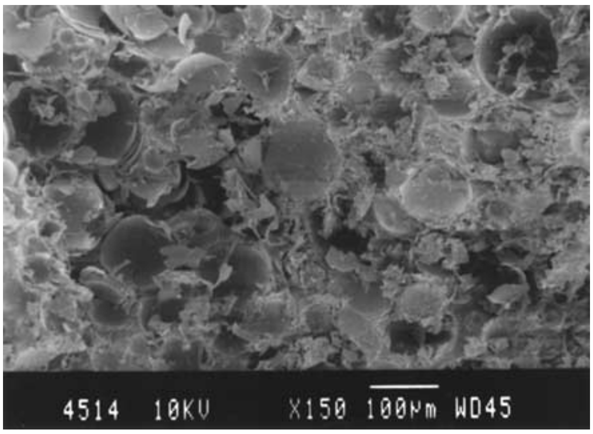

Figure 10 Scanning micrograph showing fractured pieces of microballoons in the central region of low aspect ratio (0.6) bearing compressed specimen.

A contrast in details was noted when high aspect ratio (0.91) bearing specimens were observed on the fracture plane near the corners (Fig. 11) where the crack originated. Here broken pieces of microballoons could not be seen. Microballoons, on the other hand, were seen to be fractured along definite planes without giving rise to fragments. This perhaps is a feature related to a shearing type of phenomena in the specimen. This observation supports the visual observations of early crack origination in this region and crack growth at an

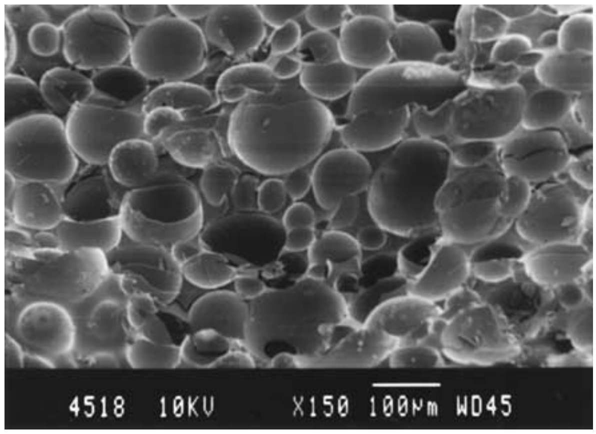

Figure 11 High aspect ratio (0.91) bearing specimen observed at a corner where the crack started. Fracture planes and fractured microballoons without the debris of microballoons can be seen in the image.

angle to the direction of the applied load. Central part of this specimen contained features quite similar to the ones observed in the Fig. 10, which are indication that the compression dominated in this region.

Scanning electron micrographs of the wedge shaped fragments separated from the sidewalls of low aspect ratio (0.6) specimens show a combination of both types of failure features, i.e. compression and shear components (Fig. 12). Similar features were observed on the fragments separated from specimen having aspect ratio of 0.4. This observation strengthens the macroscopic observations that the wedge shaped fragments separated from the sidewalls under shearing type of fracture process after initial compression. Hence, with the compression failure features, i.e. debris, shearing planes are also visible. As the separating fragments form a much smaller part than the size of the specimen, their separation does not actually make any visible effect on the load response curve.

Thus the study revealed that although the compressive yield strength values for high microballoons volume fraction syntactic foam do not vary with change in specimen aspect ratio, the response of specimen to compression changes. Microscopic observations

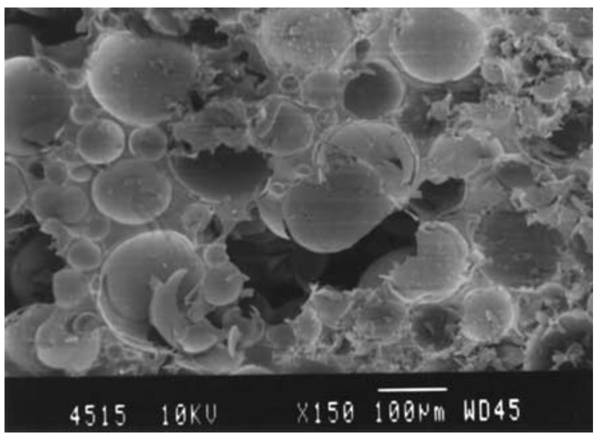

Figure 12 Low aspect ratio specimen (0.6) showing both, undamaged (top right) and fractured (right center) microballoons and also the fragments.

supported the macroscopic observations and were helpful in establishing structure-property correlation for such materials.

6. Conclusions

Shearing trends and wedge shaped crack appearance were the distinct features in the compression testing of high and low aspect ratio specimens respectively. For aspect ratio values of 0.6 or less, no distinct yield point was visible in the stress-strain curve. For the samples having aspect ratio of 0.67 or more, a marked drop after the peak stress value occurred. Based on such observations, the aspect ratio range of 0.6 to 0.67 was considered as transition one for the high microballoons volume fraction syntactic foam tested in this study. Change in specimen failure behavior suggests keeping the aspect ratio to lower values for stable compression neglecting shear stress effects.

Distinct microscopic feature of failure under compression mode in syntactic foams is the appearance of debris of microballoons on the fracture plane. Failure in shear mode does not give rise to debris. Appearance of steps in such micrographs may be due to frequent change of crack path in order to grow at an angle to the loading direction. Scanning electron microscopic examination corresponding to specimens having different aspect ratios revealed features that aided the recognition of fracture mechanisms.

Acknowledgments

The first author (N. G.) is thankful to the Chairman, Department of Metallurgy, IISC; the first and fourth (S. S.) authors are grateful to the Director, ADE for making available the facilities for the fabrication of the materials. All the authors thank Mr. C. S. Karthikeyan, Mr. Jagdish Kumar (Scientist 'C', ADE) and Mr. Govindaraju (Technical Officer 'B', ADE) for their help during the processing and the fabrication of the materials. The helpful and willing assistance of Mr. S. Sasidhara is gratefully acknowledged.

References

1. R. A. MALLOY and J. A. HUDSON, in "Intl. Encylop. of Compos.," edited by S. M. Lee (VCH, 1990).
2. M. PUTERMAN, M. NARKIS and S. KENIG, *J. Cell. Plast.* **16** (4) (1980) 223.
3. F. A. SHUTOV, "Polymeric Foams" (Carl Henser Verleg, 1991) p. 355.
4. K. ASHIDA, "Handbook of Plastic Foams" (Noyes Pub., 1995 p. 154.
5. H. J. PRICE and J. B. NELSON, *J. Compos. Mater.* **10** (1976) 314.
6. C. HIEL, D. DITTMAN and O. ISHAI, *Composites* **24** (5) (1993) 447.
7. C. ISHAI and C. HIEL, *J. Compo. Tech. and Res.* **14** (3) (1992) 155.
8. P. BUNN and J. T. MOTTRAM, *Composites* **24** (7) (1993) 585.
9. S. SANKARAN, Ph.D. thesis, Indian Institute of Science, Bangalore, India, 1997.
10. F. A. SHUTOV, *Adv. Poly. Sci.* **43** (5) (1985) 64.
11. ASTM D1621-94, "Standard Test Method for Compressive Properties of Rigid Cellular Plastics" (American Society for Testing of Materials, PA, USA).
12. ASTM D695-91, "Test Method for Compressive Properties of Rigid Plastics" (American Society for Testing of Materials, PA, USA).
13. G. E. DIETER, "Mechanical Metallurgy" (McGraw-Hill, 1988) p. 45.
14. L. S. PENN and T. T. CHIAO, "Handbook of Composites" (Van Nostrand Reinhold, 1982) p. 57.

Received 14 June 2000
and accepted 1 May 2001